

A Loaded Line 2-Bit Phase Shifter Using RF MEMS DC/Capacitive Switches

Niharika Narang*, Pranav K. Shrivastava, Ananjan Basu, and Pushpapraj Singh

Abstract—This letter presents the fabrication and measurement of a novel loaded line phase shifter design providing four different phase shifts using only two RF MEMS switches. The flexibility of choosing DC or capacitive load depending upon the phase shift required in a single RF MEMS switch makes the phase shifter compact and requires less number of proposed switches. The RF MEMS switch has been designed to provide isolation better than 10 dB in both DC and capacitive states from 16 to 45 GHz. Due to the designed RF MEMS beam switching between DC and capacitive loading, the proposed phase shifter provides a 2-bit phase shift using only two switches. The measured phase shifter has the maximum insertion loss of 0.8 dB with a bandwidth of 8 GHz from 16 to 24 GHz. The return loss is better than 10 dB for all four states. The maximum Root-Mean-Square (RMS) insertion loss error is 0.28 dB, and the phase shift error is 0.98° . The proposed phase shifter is fabricated using the surface micromachining on the sapphire substrate and occupies an area of 3.931 mm^2 .

1. INTRODUCTION

Phase shifters are crucial in phase antenna arrays for radar and telecommunication applications. Various radio frequency (RF) switches, such as field effective transistor (FET), ferrite-based switches, PIN diodes, lumped elements, loaded lines, and micro-electro-mechanical system (MEMS) switches, are used to achieve phase-shifting. RF MEMS switches offer low loss, low up-state capacitance, high linearity, and lower power consumption than other RF switches [1–4]. Moreover, RF MEMS switches can be easily integrated into the radio frequency integrated circuits (RFICs). Various analog and digital phase shifters have been discussed in the literature [5–13]. Analog-type phase shifters are more affected by noise than digital phase shifters [1]. A compact reflection-type phase shifter with 6 RF MEMS shunt switches has been used to achieve a 2-bit phase shift [5]. Phase shifters with SPnT MEMS switch and switched line require greater number of switches to achieve a given number of phase shifts, and several Metal-Insulator-Metal (MIM) capacitors provide a 2-bit phase shift requiring an area of 5 mm^2 [6, 7]. A 2-bit phase shift is obtained using distributed microelectromechanical transmission-line (DMTL) type phase shifter [8, 11]. All these phase shifters require a large number of MEMS switches; therefore, the area of the phase shifter increases.

To design a compact RF MEMS phase shifter offering a large number of phase shifts using a lower count of switches, along with enhanced performance and reduced circuit complexity, is most desired in RFICs. This paper presents a novel 2-bit phase shifter having four different phase shifts (center frequency is 20 GHz) consisting of only two RF MEMS switches. The RF MEMS DC/Capacitive switch (integrated into the designed phase shifter) can be switched between capacitive and DC loads. It gives a 2-bit fine phase shift of 0° , 5.625° , 11.25° , and 22.5° . The maximum insertion loss in phase shifts is less than 0.8 dB. This phase shifter offers a return loss of better than 10 dB from 16 GHz to 24 GHz.

Received 18 February 2023, Accepted 15 May 2023, Scheduled 13 June 2023

* Corresponding author: Niharika Narang (Niharika.Narang@care.iitd.ac.in).

The authors are with the Centre for Applied Research in Electronics (CARE), IIT Delhi, 110016, India.

2. DEVICE DESIGN

Loaded line phase shifter provides low loss, compact size, and high performance. These phase shifters provide acute phase shifting [1]. In this article, transmission lines are loaded using MEMS switches to provide phase shifting of 5.625° , 11.25° , and 22.5° . The schematic of the designed RF MEMS 2-bit phase shifter is presented in Fig. 1. Two RF MEMS switches are used to provide either capacitive loading or ground to the transmission lines. The center transmission line 1 is unloaded. However, transmission lines 2 and 3 are loaded with other transmission lines and MEMS switches. Fig. 1(a) shows that transmission line 2(3) is loaded with transmission line 5(4). Transmission lines 4 and 5 are loaded with the RF MEMS DC/Capacitive switches 1 and 2.

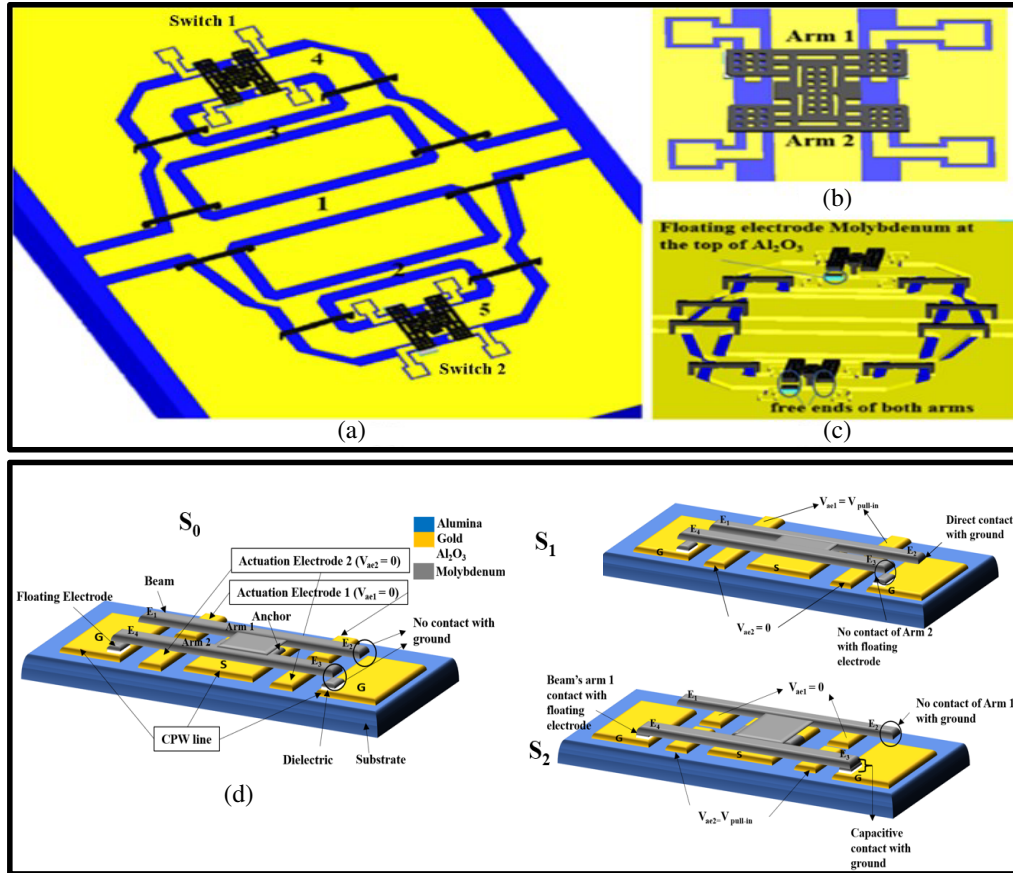


Figure 1. (a) Front view of the proposed 2-bit phase shifter. (b) RF MEMS DC/capacitive switch integrated into the proposed design. (c) Side view of the designed phase shifter. (d) Working principle of RF MEMS DC/capacitive switch in various states.

2.1. RF MEMS DC/Capacitive Switch Design

The RF MEMS DC/Capacitive switch (given in Fig. 1(b)) is connected at the center of the coplanar waveguide (CPW) signal line through two anchors only. This designed switch consists of two completely free arms Arm 1 and Arm 2. Arm 1(2) has two ends E_1 and E_2 (E_3 and E_4). The molybdenum-Al₂O₃ layer is deposited on both the ground planes below E_3 and E_4 , whereas no such layer is present below E_1 and E_2 . This switch can operate in three states (as shown in Fig. 1(d)): OFF state (S_0), DC-ON state (S_1), and Capacitive-ON state (S_2). The design remains in S_0 when no pull-in voltage is given on any of the actuation electrodes. S_1 can be achieved by applying pull-in voltage (V_{ae1}) to actuation electrodes below E_1 and E_2 . S_2 can be achieved by applying pull-in voltage (V_{ae2}) to actuation electrodes below

E_3 and E_4 . However, for the proposed phase shifter, only capacitive-ON and DC-ON states are the required states, and the OFF state is the unused state. Molybdenum is used as a switching material to provide robustness against stress and temperature variations [9]. In the S_1 state, E_1 and E_2 ends will directly contact the ground plane. However, in the S_2 state, E_3 and E_4 will touch the bottom molybdenum- Al_2O_3 gold layer to make capacitive contact with the ground. Molybdenum (as a floating electrode) on the top of Al_2O_3 provides fixed capacitance during contact. The switch is designed so that when Arm 1 moves down due to pull-in voltage, Arm 2 moves up and vice versa. This switch can shift between capacitive load and DC ground load. Hence, this can be used in phase shifters. Conventionally for a 2-bit phase shifter having four different states, more than two switches are required. Only two RF MEMS DC/Capacitive switches have been used in the proposed phase shifter to obtain these states.

2.2. Equivalent Circuit of the Phase Shifter

The equivalent circuit of the designed phase shifter is shown in Fig. 2. Here, Z_0 is the characteristic impedance of the transmission lines 1, 4, and 5. Z_1 is the characteristic impedance of transmission lines 2 and 3. C_1 and C_2 are the capacitances due to the capacitive ends of proposed switches 1 and 2. θ is the electrical length of transmission lines. The effective phase shifts provided by the switches in various states are given in Table 1. Hence, the proposed phase shifter offers 2-bit phase shifts using only two RF MEMS switches.

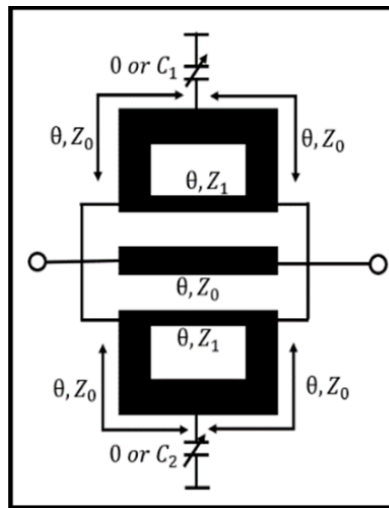


Figure 2. Equivalent circuit of RF MEMS phase shifter.

Table 1. Various states in the proposed phase shifter.

State	Effective capacitance provided by RF MEMS switches		Phase	Desired Phase Shift
	Switch 1	Switch 2		
PS0	0 (S_1)	0 (S_1)	θ_1 (reference)	0°
PS1	C_1 (S_2)	0 (S_1)	θ_2	$5.625^\circ (\theta_2 - \theta_1)$
PS2	0 (S_1)	C_2 (S_2)	θ_3	$11.25^\circ (\theta_3 - \theta_1)$
PS3	C_1 (S_2)	C_2 (S_2)	θ_4	$22.5^\circ (\theta_4 - \theta_1)$

* C_1, C_2 : Capacitive loading to the ground (using the first arm), 0: Direct contact with the ground (using the second arm)

The approximate analysis of phase θ_4 in PS₃ state (when switch 1 provides capacitance C_1 and switch 2 provides capacitance C_2) is calculated by using $ABCD$ and admittance matrix and is given as:

$$ABCD_{Tl_{51}} = ABCD_{Tl_{52}} = \begin{bmatrix} 0 & iZ_0 \\ i/Z_0 & 0 \end{bmatrix} \quad (1)$$

where Tl_{51} and Tl_{52} transmission lines have a length half of the transmission line 5. $ABCD_{Tl_{51}}$, $ABCD_{Tl_{52}}$, and $ABCD_{C_2}$ are the $ABCD$ parameters for transmission lines and capacitor C_2 .

$$ABCD_{C_2} = \begin{bmatrix} 1 & 0 \\ i\omega C_1 & 1 \end{bmatrix} \quad (2)$$

$$ABCD_{f_2} = ABCD_{Tl_{51}} * ABCD_{C_2} * ABCD_{Tl_{52}} \quad (3)$$

$ABCD_{f_1}$ is the total $ABCD$ parameter equivalent of the cascading of Tl_{51} , C_2 , and Tl_{52} . Admittance matrix Y_{f_2} can be extracted by converting (3) to Y parameters. Similarly, Y_{f_1} can be calculated using (1)–(3) again for capacitance C_1 and transmission line sections Tl_{41} and Tl_{42} . The total admittance matrix (Y_t) from the input port to the output port is given by:

$$Y_t = Y_{f_1} + Y_{Tl_2} + Y_{Tl_1} + Y_{Tl_3} + Y_{f_2} \quad (4)$$

S_{21} can be calculated by converting (4) to a scattering matrix and is given as:

$$S_{21} = -\frac{2Z_0 \left(-\frac{i}{C_1\omega Z_0^2} - \frac{i}{C_2\omega Z_0^2} + \frac{i}{Z_0} + \frac{2i}{Z_1} \right)}{\left(1 + \left(-\frac{i}{C_1\omega Z_0^2} - \frac{i}{C_2\omega Z_0^2} \right) Z_0 \right)^2 - Z_0^2 \left(-\frac{i}{C_1\omega Z_0^2} - \frac{i}{C_2\omega Z_0^2} + \frac{i}{Z_0} + \frac{2i}{Z_1} \right)^2} \quad (5)$$

S_{21} phase = θ_4 can be calculated using (5) and is given as:

$$\theta_4 = \tan^{-1} \left(\left(1 + \frac{2 * Z_0}{Z_1} \right) - \left(\frac{2Z_0^2}{Z_1^2} + \frac{2Z_0Z_1}{Z_1^2} + 1 \right) \left(\frac{C_1C_2}{C_1 + C_2} \right) \omega Z_0 \right) \quad (6)$$

Similarly, the scattering matrix and hence, phase in θ_1 , θ_2 and θ_3 in states PS, PS₁, and PS₂, respectively, can be calculated using Table 1 and (1)–(5):

$$\theta_1 = -90^\circ \quad (7)$$

$$\theta_2 = \tan^{-1} \left(\left(1 + \frac{2Z_0}{Z_1} \right) - \left(\frac{2Z_0^2}{Z_1^2} + \frac{2Z_0Z_1}{Z_1^2} + 1 \right) C_1\omega Z_0 \right) \quad (8)$$

$$\theta_3 = \tan^{-1} \left(\left(1 + \frac{2 * Z_0}{Z_1} \right) - \left(\frac{2Z_0^2}{Z_1^2} + \frac{2Z_0Z_1}{Z_1^2} + 1 \right) C_2\omega Z_0 \right) \quad (9)$$

The values of the capacitances C_1 and C_2 are chosen to provide the desired phase shift at $Z = 50 \Omega$ and $\theta = 90^\circ$, $Z_1 = 70.7 \Omega$ (calculated using odd-even analysis).

2.3. Fabrication

The fabrication process of the designed phase shifter is simple and requires only four masks. Surface micromachining is used to design the proposed RF MEMS switch. Sapphire is used as a substrate to design the phase shifter. 300 nm thick gold lines are deposited and patterned to form a CPW transmission line. Aluminum oxide (Al_2O_3) is used as the dielectric material. Thin molybdenum is used as a floating electrode on top of aluminum oxide. Mo/ Al_2O_3 (70 nm/100 nm) are deposited and patterned. 500 nm thick molybdenum has been used as beam material to provide robustness against stress and temperature. The sacrificial layer (Silicon dioxide, 1 μ m thick) is deposited on the bottom layer, and anchors are patterned between the top beam and bottom part. Figs. 3(a) and 3(b) show the detailed process flow of the fabrication.

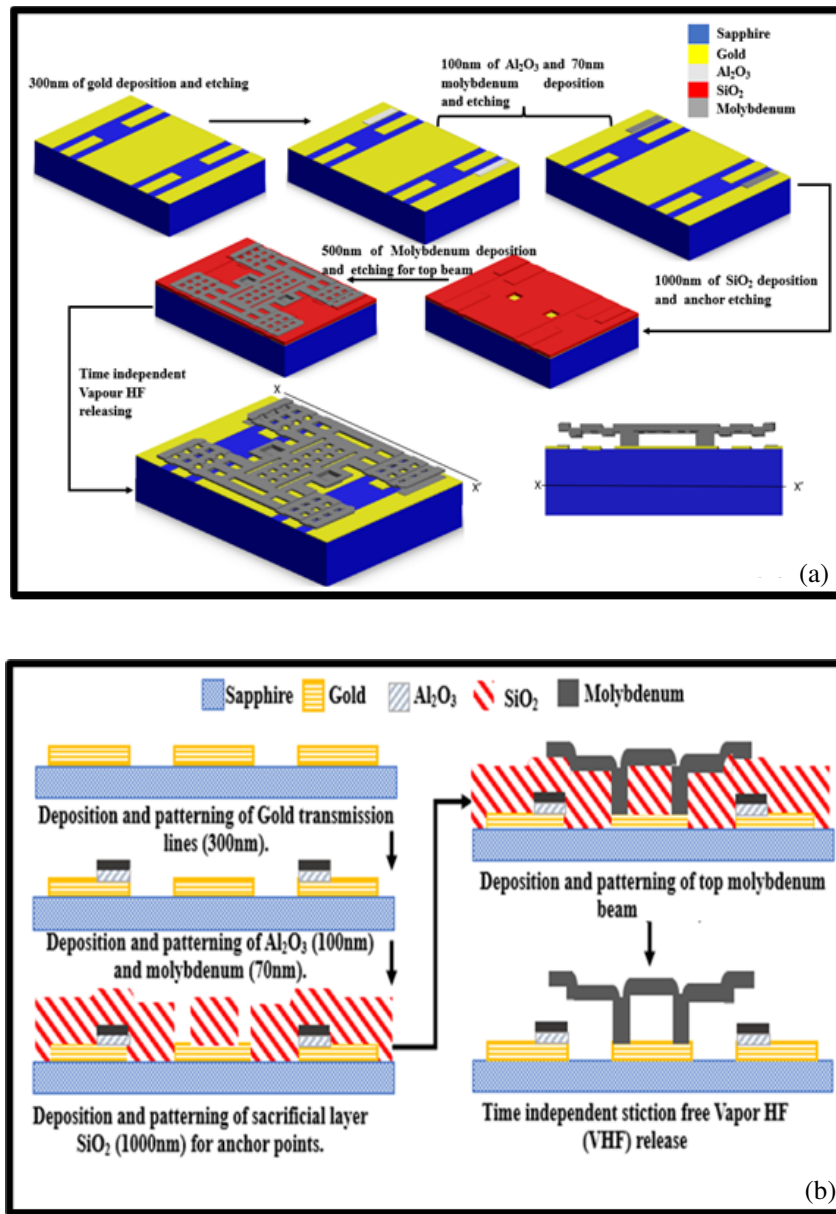


Figure 3. (a) 3-D top-down. (b) 2-D side view of the fabrication flow of the proposed device.

3. RESULTS AND DISCUSSIONS

This proposed phase shifter is designed to provide a 2-bit phase shift using novel RF MEMS DC/capacitive switches. The length of each arm in the switch is $228\ \mu\text{m}$, and the total width of the switch is $180\ \mu\text{m}$. CPW transmission lines 1, 4, and 5 have characteristics impedance $50\ \Omega$ ($50\ \mu\text{m}/110\ \mu\text{m}/5\ \mu\text{m}$), whereas transmission lines 2 and 3 have characteristics impedance $70.7\ \Omega$ ($50\ \mu\text{m}/31.2\ \mu\text{m}/50\ \mu\text{m}$). RF MEMS switches are integrated at the center of transmission lines 4 and 5. The total area of anchors in each switch is $180\ \mu\text{m}^2$. The DC characteristics of the proposed switch are simulated in CoventorWare. Fig. 4 authenticates that molybdenum offers higher robustness than gold against temperature and residual stress (at room temperature). The area of the floating electrode and dielectric (deposited on the ground plane below E_3 and E_4) in switch 1(2) is $372(220)\ \mu\text{m}^2$. The area of the floating electrode chosen to provide net capacitance in switch 1(2) during the capacitive

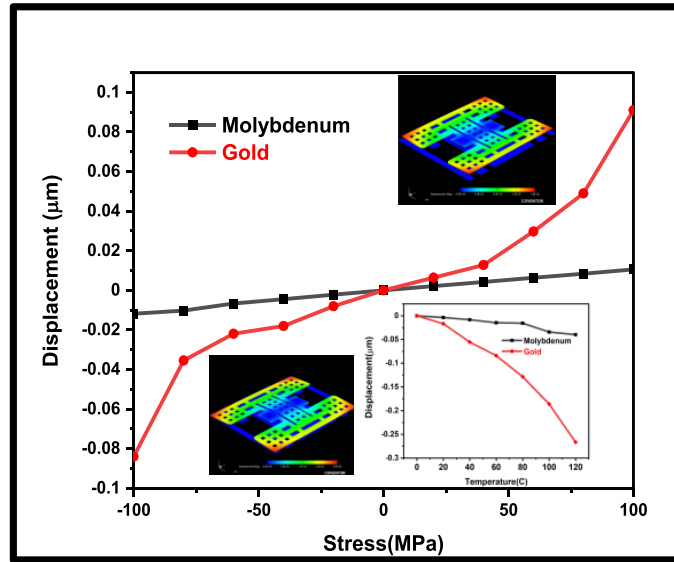


Figure 4. Deflection in the RF MEMS DC/capacitive switch due to temperature and stress variations.

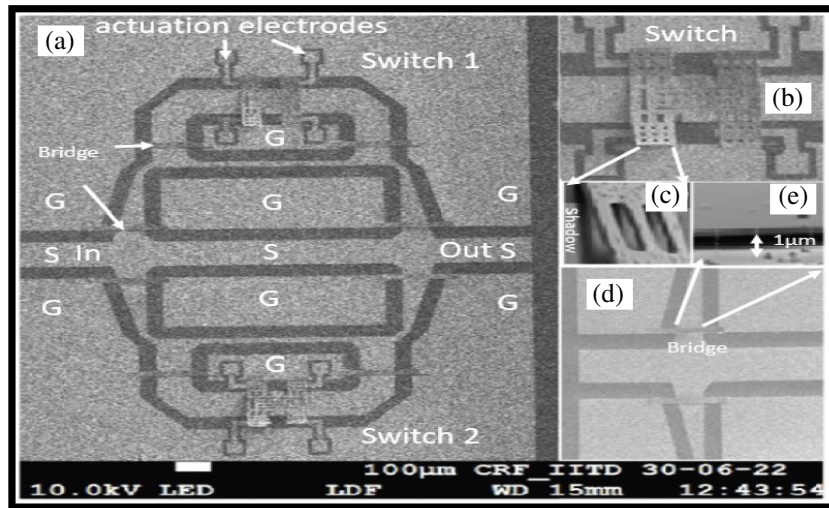


Figure 5. Scanning electron microscope (SEM) image of the (a) proposed phase shifter, (b) RF MEMS DC/capacitive switch, (c) detailed view of the released switch arm with shadow (curled up due to residual stress), (d) grounds connected with the inner ground plane using bridges, (e) detailed view of the bridges showing gap from the bottom plane.

down state is 0.586 pF (0.347 pF). The pull-in voltage of the switches is 7.5 V, and the lift-off voltage is 5.85 V. The dielectric constant of deposited Al_2O_3 is 8.9. The insertion phase is calculated in each state using (6)–(9). The net calculated phase shifts are 0° , 5.625° , 11.25° , and 22.5° . The RF performance of the designed phase shifter is analyzed in Ansys (HFSS). The proposed phase shifter and RF MEMS switch are fabricated (shown in Fig. 5), and the RF characteristics are measured using a CASCADE probe station SUMMIT 1100 equipped with Agilent E8361C PNA Network Analyzer (10 MHz–67 GHz) (as shown in Fig. 6). DC voltage sources (DC1 and DC2) are used to provide actuation voltages to the designed RF MEMS switch. The pitch of the infinity probes (GSG) was 150 μm . Calibration has been done on the impedance standard substrate (ISS) wafer using the short-open-load-through (SOLT) method. The measured RF performance of the DC/capacitive RF MEMS switch is shown in Figs. 7(a)



Figure 6. RF performance measurement setup for device under test (DUT).

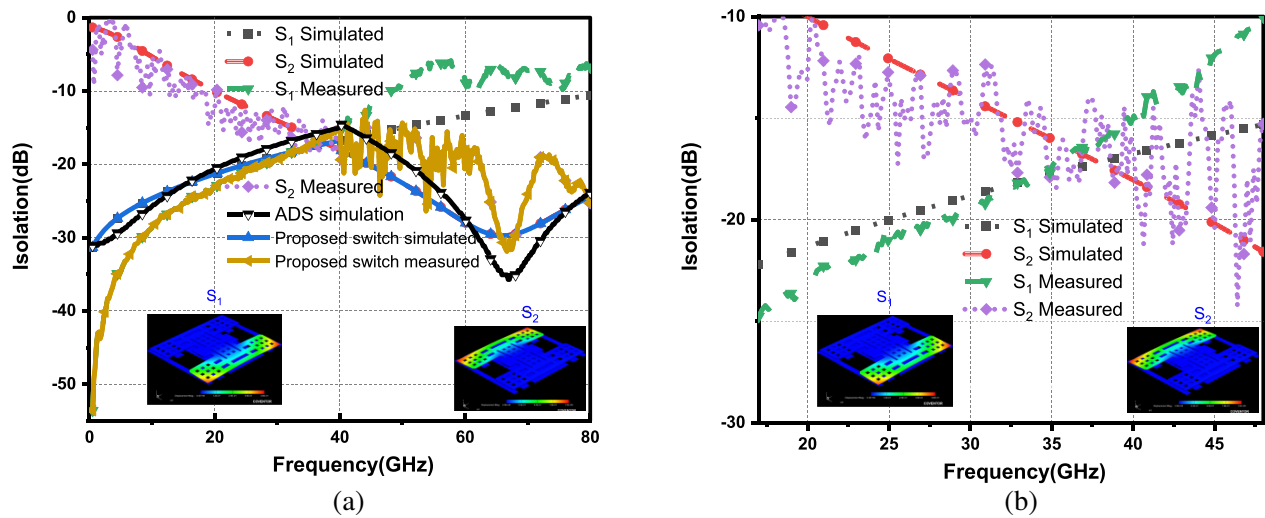


Figure 7. (a) S parameters comparison of RF MEMS switch during on-states S_1 and S_2 from DC-80 GHz (along with Advance Design System (ADS) simulation). (b) Isolation better than 10 dB from 16–45 GHz in the designed RF MEMS switch.

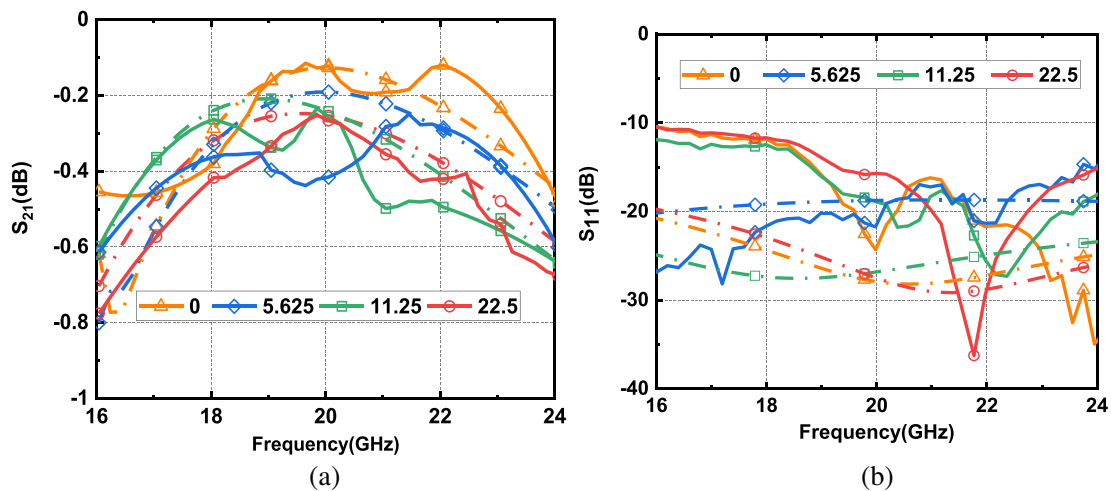


Figure 8. Proposed phase shifter S parameter comparison, (a) S_{21} magnitude, (b) S_{11} magnitude (Simulated (dash) and measured (solid)).

4. CONCLUSIONS

The design, fabrication, and measurement of the proposed RF MEMS 2-bit phase shifter have been presented in this article. The designed RF MEMS DC/capacitive switch provides fixed capacitance due to the floating electrode and can switch between capacitive and DC loads. The fabrication process of the designed phase is simple and requires only four masks. Measurement results authenticate the novel design of phase shifter with unique RF MEMS DC/Capacitive switches that provide high RF performance in each state with a maximum RMS phase shift error of 0.98° , an RMS gain error of less than 0.28 dB, and a return loss better than 10 dB.

REFERENCES

1. Rebeiz, G. M., *RF MEMS: Theory, Design, and Technology*, 3rd Edition, 259–290, John Wiley & Sons, New Jersey, USA, 2003.
2. Qing, Z. Y., L. Han, L. F. Wang, J. Y. Tang, and Q. A. Huang, “A novel three-state RF MEMS switch for ultrabroadband (DC–40 GHz) applications,” *IEEE Electron Device Letters*, Vol. 34, No. 7, 1062–1064, 2013, <http://doi.org/10.1109/LED.2013.2269993>.
3. Afrang, O. R., S. Afrang, and A. A. Hamzah, “Very small size capacitive DMTL phase shifters using a new approach,” *Microsystem Technologies*, Vol. 28, No. 8, 2107–2122, 2022, <http://doi.org/10.1007/s00542-022-05354-0>.
4. Guo, L., H. Zhu, and A. Abbosh, “Wideband phase shifter with wide phase range using parallel coupled lines and L-shaped networks,” *IEEE Microwave and Wireless Components Letters*, Vol. 26, No. 7, 592–594, 2016, <http://doi.org/10.1109/LMWC.2016.2587833>.
5. Kim, H. T., J. H. Park, J. Yim, Y. K. Kim, and Y. Kwon, “A compact V-band 2-bit reflection-type MEMS phase shifter,” *IEEE Microwave and Wireless Components Letters*, Vol. 12, No. 8, 324–326, 2002, <http://doi.org/10.1109/LMWC.2002.803198>.
6. Müller, D., P. Pahl, A. Tessmann, A. Leuther, T. Zwick, and I. Kallfass, “A WR3-band 2-bit phase shifter based on active SPDT switches,” *IEEE Microwave and Wireless Components Letters*, Vol. 28, No. 8, 810–812, 2018, <http://doi.org/10.1109/LMWC.2018.2853085>.
7. Gong, S., H. Shen, and N. S. Barker, “A 60-GHz 2-bit switched-line phase shifter using SP4T RF-MEMS switches,” *IEEE Transactions on Microwave Theory and Techniques*, Vol. 59, No. 4, 894–900, 2011, <http://doi.org/10.1109/TMTT.2011.2112374>.
8. Unlu, M., S. Demir, and T. Akin, “A 15–40-GHz frequency reconfigurable RF MEMS phase shifter,” *IEEE Transactions on Microwave Theory and Techniques*, Vol. 61, No. 7, 2865–2877, 2013, <http://doi.org/10.1109/TMTT.2013.2271995>.
9. Kumar, S., D. S. Arya, and P. Singh, “Volatile or non-volatile switching? Establishing design parameters for metal-contact relays using ON/OFF hysteretic behavior (RT to 300°C),” *Applied Physics Letters*, Vol. 118, No. 1, 0135051–5, 2021, <http://doi.org/10.1063/5.0025062>.
10. Shrivastava, P. K., S. K. Koul, and M. P. Abegaonkar, “Compact K-band lange coupler based 2-bit RF MEMS reflection-type phase shifter,” *2018 IEEE MTT-S International Microwave and RF Conference (IMaRC)*, 1–4, 2018, <http://doi.org/10.1109/IMaRC.2018.8877134>.
11. Prithivirajan, V., P. Venkatakrisnan, and A. Punitha, “Low loss 2-bit distributed MEMS phase shifter using chamfered transmission line,” *Indian Journal of Science and Technology*, Vol. 8, No. 5, 510–517, 2015, <http://doi.org/10.17485/ijst/2015/v8i6/70112>.
12. Hu, J., Y. Li, and Z. Zhang, “A novel reconfigurable miniaturized phase shifter for 2-D beam steering 2-bit array applications,” *IEEE Microwave and Wireless Components Letters*, Vol. 31, No. 4, 381–384, 2021, <https://doi.org/10.1109/LMWC.2021.3057223>.
13. Li, X., K. Y. Chan, and R. Ramer, “E-band RF MEMS differential reflection-type phase shifter,” *IEEE Transactions on Microwave Theory and Techniques*, Vol. 67, No. 12, 4700–4713, 2019, <https://doi.org/10.1109/TMTT.2019.2944623>.